Advances in the high bootstrap fraction regime on DIII-D towards the Q=5 mission of ITER steady state

J.P. Qian[1], A.M. Garofalo[2], X. Z. Gong[1], Q.L.Ren[1], S. Y. Ding[1], W.M. Solomon[3], G. S. Xu[1], B.A. Grierson[3], W. F. Guo[1], C.T. Holcomb[4], J. McClenaghan[5], G.R. McKee[6], C. K. Pan[1], G.M. Staebler[2], B. N. Wan[1]

[1] Institute of Plasma Physics, Chinese Academy of Science, Hefei, China
[2] General Atomics, San Diego, USA
[3] Princeton Plasma Physics Laboratory, Princeton, New Jersey, USA
[4] Lawrence Livermore National Laboratory, Livermore, California, USA
[5] Oak Ridge Associated Universities, Oak Ridge, TN, USA
[6] University of Wisconsin-Madison, Madison, Wisconsin, USA

Abstract. Recent EAST/DIII-D joint experiments on the high poloidal beta β_P regime in DIII-D have extended operation with internal transport barriers (ITBs) and excellent energy confinement ($H_{98y2} \sim 1.6$) to higher plasma current, for lower $q_{95} \leq 7.0$, and more balanced Neutral Beam Injection (NBI) (torque injection <2 Nm), for lower plasma rotation relative to previous results [Garofalo et al., IAEA 2014, Gong et al., IAEA 2014]. Transport analysis and experimental measurements at low toroidal rotation suggest that the ExB shear effect is not key to the ITB formation in these high β_P discharges. Experiments and TGLF modeling show that the Shafranov shift has a key stabilizing effect on turbulence. Extrapolation of the DIII-D results using a 0-D model shows that with the improved confinement, the high bootstrap fraction regime could achieve fusion gain Q=5 in ITER at $\beta_N \sim 2.9$ and $q_{95} \sim 7$. With the optimization of q(0), the required improved confinement is achievable when using 1.5-D TGLF-SAT1 for transport simulations. Results reported in this paper suggest that the DIII-D high β_P scenario could be a candidate for ITER steady state operation.

1. Introduction

Previous EAST/DIII-D joint experiments on the high poloidal beta regime in DIII-D have developed fully non-inductive plasmas with internal transport barriers (ITBs) at large minor radius ($\rho \geq 0.6$), excellent energy confinement quality ($H_{98y2} \sim 1.6$), and high bootstrap current fraction ($f_{BS} > 80\%$) at high $q_{95} \sim 12$ [1-3], whereas $q_{95} \sim 5$ is envisaged for ITER steady state [4]. Therefore, it is necessary to develop a scenario at lower q_{95} with the merits of high bootstrap fraction and good energy confinement to contribute to ITER steady state. In addition, scenarios at low plasma rotation should also be addressed since it is expected to be difficult to drive high toroidal rotation in ITER with present Neutral Beam Injection (NBI) torque [5].

In the 2015-2016 DIII-D experimental campaign, the extension of the high poloidal beta scenario towards low plasma rotation and q_{95} relevant to steady state operation at Q=5 in ITER has been carried out. The high poloidal beta scenario was

extended inductively to higher plasma current, for lower q_{95}, and more balanced neutral beam injection (NBI), for lower plasma rotation. The experimental results have shown that the key feature of large radius ITB, which results in excellent energy confinement characteristic, is maintained in the extended operational regimes.

The paper is organized as follows. Section 2 presents the extension of high bootstrap fraction scenarios toward low plasma rotation and the understanding of high performance at low rotation. Section 3 describes the high bootstrap scenario at q_{95} relevant to ITER steady state, showing that good confinement with ITBs can be maintained at lower q_{95}, leading to the high performance. Adaptation of DIII-D high bootstrap current fraction scenario to ITER steady state using 0-D and 1.5 transport modeling is discussed in section 4. Finally, a brief summary is given in section 5

2. Extension of high bootstrap fraction scenarios toward low plasma rotation for ITER steady state operation

A high q_{95} with high f_{BS} fraction discharge was chosen as the reference to extend to the low plasma rotation regime. The early NB heating was utilized during the Ip ramp-up phase to heat the plasma and delay the penetration of inductive current together with the optimization of gas puffing, to produce the desirable q profile ($q_{min}>2.0$). The β_N was increased with feedback control using the neutral beam power. The low rotation plasma was gradually obtained by increasing the counter-Ip NB power from shot to shot for a more balanced momentum injection. Meanwhile, the plasma density and plasma wall separation were carefully optimized to reduce the fast ion losses from low plasma current operation and avoid wall overheating by the lost fast ions.
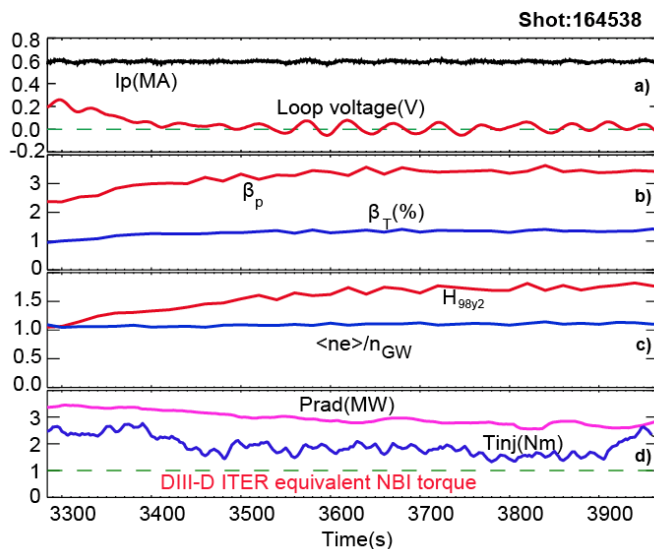

FIG. 1. time traces of several plasma parameters for representative low toroidal roataion discharge 164538; a) plasma current, loop voltage; b) β_N and β_T ;c) H_{98y2} and $<ne>/n_{GW}$; d) radiation power, NBI torque. The green dashed line is the DIII-D ITER equivalent NBI torque.

Typical waveforms of the low toroidal rotation discharge with the high f_{BS} are shown in figure 1. The plasma configuration is double null. Plasma parameters are as follows: plasma current Ip=0.6MA, toroidal magnetic field B_T=2.1T, major radius R=1.65m, minor radius a=0.58m, elongation k=1.9, q_{95}~12. The normalized β_N ~3.0 and β_T ~1.45% were achieved. Loop voltage decreased to nearly zero and was kept nearly constant, which indicates the nearly full noninductive current drive

condition. A high H_{98y2} of 1.7 was achieved owing to the large radius ITB in the electron temperature and density profiles and ion temperature and rotation profiles, with electron density at Greenwald density fraction ~1.0-1.1. It should be mentioned that no strong impurity accumulation was observed even with high confinement.

This low rotation discharge exhibits similar excellent energy confinement quality when compared to the previous high rotation discharge in the 2014 campaign experiement [1]. Figure 2 shows the profiles of electron temperature T_e and rotation profiles with different torque (~1.8Nm for 164538 and ~5.0 Nm for 163791), and turbulence measurements from beam emission spectrosciopy (BES). A T_e profile with steep ITB at large minor radius, ρ~0.6, and no measurable turbulence at that radius or indside are obtained at both high and low plasma rotation. The ITB foot in the rotation profile is observed at smaller minor radius with reduced NBI torque, but the ITB foot in the Te profile is unchanged. These observations suggest that the shear in the toroidal rotation does not play a role in the formation of the ITB.

Here the ion energy transport is analyzed. The electron temperature，electron density and toroidal rotation profiles are fixed and only the ion temperature profile is predicted by TGYRO[6] with TGLF[7]+NEO[8] to investigate the ion channel energy transport.
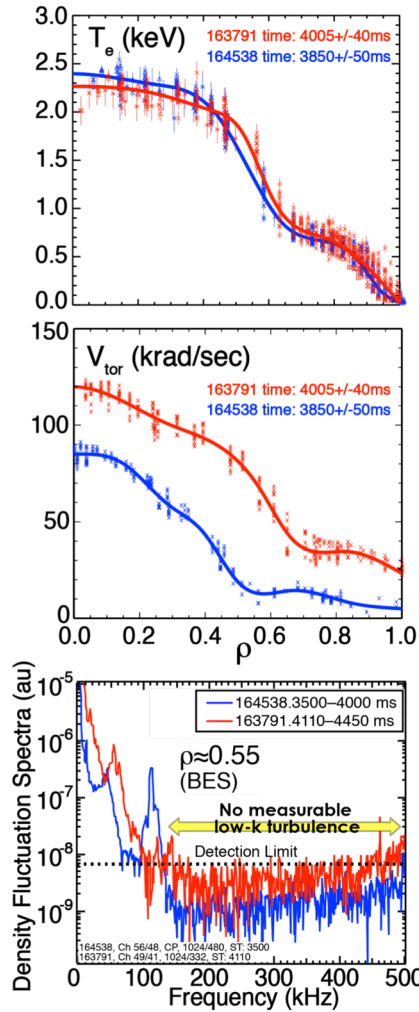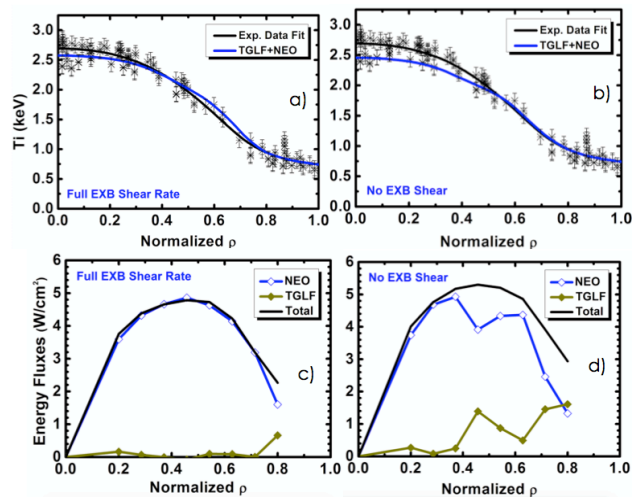

FIG. 2. Comparsion of radial electron temperature and rotation profiles for the high and low NBI torque discharges, and of low-k density fluctuations spectra.

The modeling shows little sensitivity on toroidal rotation and the predicted ion temperature agrees well with the experimental data with or

FIG. 3. Simulations of ion temperature amd ion energy flux profiles from the experimental data fit (black line) and the TGYRO predictions (blue line) with and without EXB shear rate for the DIII-D high β_P discharge 154372 at 4000ms.

without ExB shear as shown in figure 3 (a-b). Meanwhile, the ion energy fluxes predicted by TGLF and NEO as shown in figure 3(c-d) show that the neoclassical transport dominates the ion thermal transport. The turbulent ion energy flux increases slightly as shown in figure 3(d) when EXB flow shear effect is turned off, but still remains much smaller than the neoclassical energy flux.

This low rotation scenario could be attractive for ITER. According to the equivalence definition in Ref. [5], the DIII-D NBI torque equivalent to the ITER NBI torque is ~3% of the actual NBI torque on ITER, i.e. ~1 Nm for this high beta scenario. In another, more transient, DIII-D discharge, the reduced NBI torque (~1.1 Nm for discharge 163552), comes very close to the equivalent ITER torque, still with excellent energy confinement. The low rotation experiments presented in this paper have increased confidence in the potential of low rotation plasmas with good confinement for ITER steady state operation.

3. Development of high bootstrap scenario at q_{95} relevant to ITER steady state

In the recent experiment, another scenario extension towards ITER steady state relevant q_{95} has been explored by adding a second Ip ramp-up in the discharge evolution. The onset of the second Ip ramp-up begins after a high performance plasma equilibrium with ITB was established. The plasma current ramp-up rate (dIp/dt) was fixed to ~0.2MA/s.

Figure 4 shows time histories of several parameters for two representative high beta discharges in the development of lower q_{95} (~0.8MA for 164504 and ~1MA for 164510). The low q_{95} waveform was obtained by increasing plasma current from shot to shot with the β_N ~2.8 utilizing NBI power feedback control. The use of total
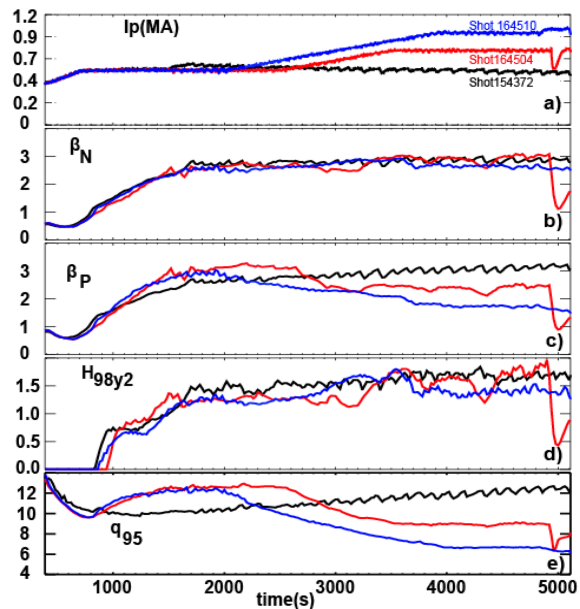

FIG. 4. Time histories of several plasma parameters for two representative high beta discharges for the development of lower q_{95}. From a) to e) plasma current, normalized β_N, poloidal β_P, confinement H_{98y2} and q_{95}.

heating and current drive power is ~ 11MW for discharge 164510. The minumum q_{95}~6.0 was obtained with 1MA plasma current.

The q profile is weak shear with the q_{min}>2.0 infered from the EFIT code [9] constrained by MSE measurement. The q(0) was almost unchanged by the second plasma current ramp-up. In these discharges, the internal inductance, li decreases from 0.8 to 0.6 with increasing plasma current, which is consistent with the expectation that the ohmic current may be "frozen" at large minor radius, outside the hot ITB core, for several current profile relaxation times (τ_R~1 s).

This high plasma current discharge 164510 also exhibits excellent energy confinement quality with the $H_{98y2}>1.5$ before 3.7s. The high performance is associated with the formation of large radius ITB ($\rho\sim0.7$). It is observed that the core
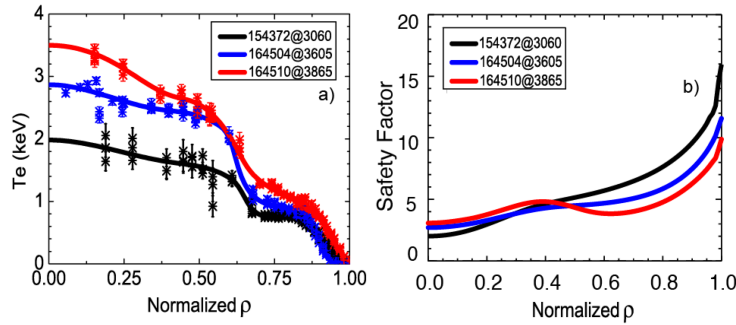

FIG. 5. Overlay of electron temperature profiles and q profiles.

electron temperature goes up when comparing with two other T_e profiles at lower Ip. With increasing Ip, the location of the ITB is nearly unchanged, as can be seen from the electron temperature profiles in figure 5a. It is also worth pointing out that the ITB became weaker at higher plasma current, with a higher T_e pedestal. With plasma current appoaching 1 MA, the ITB becomes very weak, resulting in a final drop of the performance (H_{98y2} from 1.6 to 1.3).

This gradual weakening and final disappearance of the ITB may relate to a Shafranov shift effect on the transport, which was reported in [10]. To investigate the Shafranov shift effect on the transport for the high β_P discharges, the ion turbulent energy fluxes was calculated by TGLF for a sequence of synthetic equilibria, which
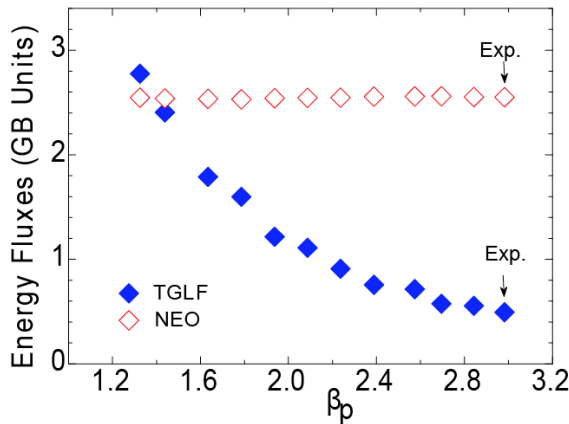

FIG. 6 Ion turlent and neoclassical energy fluxes calculated with TGLF and NEO versus β_P.

are generated by scaling down the pressure profile from an experimental reconstruction while holding the plasma shape and the q profile nearly fixed. The turbulent energy fluxes calculated by TGLF at $\rho=0.63$, which is in the ion-ITB region, increase gradually with the decrease of β_P, as shown in figure 6. The energy fluxes calculated by NEO are also shown in figure 6, which is not sensitive to β_P. This study shows that the Shafranov shift has a stabilizing effect on the energy turbulent transport in this discharge. This helps explain why the ITB could be maintained for the high β_P discharges with low toroidal rotation. Recent experiments have confirmed these TGLF predictions: in a discharge where the poloidal beta was deliberately reduced by reducing the heating power, it is observed that the ITB persists from $\beta_P\sim3$ down to $\beta_P\sim1.8$, where TGLF predicts turbulent transport becomes comparable to neoclassical. Turbulence measurements show that the ion-scale fluctuations indeed increase as beta is reduced, as illustrated in Fig. 7.
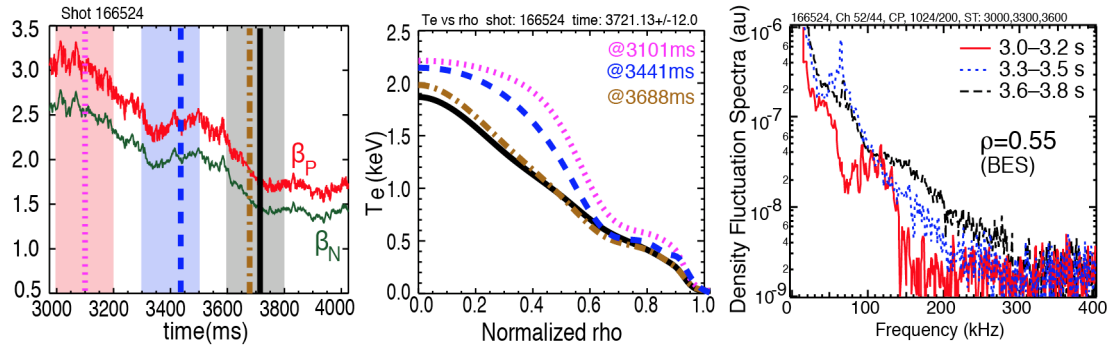
FIG. 7. Time history of β_P for discharge 166524 and Te profile at several timeslices with different β values. Turbulence measurements for different time ranges during the β scan.

The recent experimental results of the exploration of lower q_{95} and lower plasma rotation are summarized in the plots of H_{98y2} versus q_{95} and rotation at $\rho = 0.5$ in figure 8. High values of H_{98y2} are associated with presence of large radius ITB. In the DIII-D experiments, reducing q_{95} as well as reducing the NB torque results in reducing the non-inductive fraction below 1. The plots show that large radius ITBs can be maintained at significantly reduced values of q_{95} and of the plasma rotation, compared to earlier experiments [1].
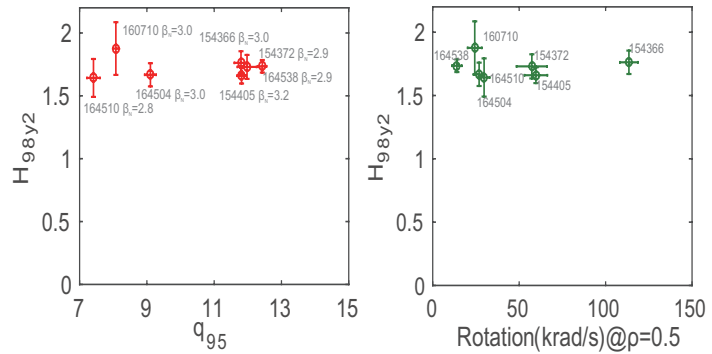
FIG. 8. Normalized confinement quality (H_{98y2}) versus q_{95} and plasma rotation at mid-radius for high q_{min}, high poloidal and normalized β, ITER steady state demonstration plasmas, where the error bar is the standard deviation over the period of two energy confinement times.

4. Extrapolating the DIII-D high bootstrap, high β_P scenario towards the Q=5 mission of ITER steady state

The DIII-D results provided in this paper have many of the desired characteristics necessary for the Q=5 fusion performance mission of the ITER steady state scenario including good normalized confinement ($H_{98y2} \sim 1.6$), high on-axis Greenwald fraction up to ($f_{gr} \sim 1.2$), and high bootstrap fraction($f_{BS} \sim 80\%$). Using similar limits to the Greenwald fraction and normalized confinement, we use a 0-D model [11] to extrapolate a high bootstrap fraction scenario to ITER with $B_T=5.3T$ and a day one auxiliary heating power of 73MW. The shape of the density and temperature profiles are the same as a recent DIII-D high β_P scenario. The total plasma current for noninductive operation increases with higher β_N since the bootstrap fraction is fixed

at $f_{BS}\sim80\%$, resulting in the decrease of q_{95} (see Fig. 9). This 0-D modeling analysis indicates that fully non-inductive operation at $\beta_N\sim2.9$ and $q_{95}\sim7$ (plasma current ~7.4MA) could achieve the Q=5 mission of ITER steady state.

To validate the hypothesis of high core confinement, $H_{98y2}\sim1.6$, an improved TGLF-SAT1 1.5-D transport model [12], which includes zonal flow regulation of multi-scale turbulence, has been used. An example of alignment of simulations with the experimental profiles in [3] suggests that TGLF-SAT1 is an adequate predictive model. One time slice of n_e, T_e, T_i and q profiles with an ITB from DIII-D high beta scenarios scaled up to ITER using the 0-D modeling are presented in Figure 10. The temperature and density profiles are then evolved using TGYRO with TGLF-SAT1 and assuming no ExB shear. Figure 10 shows the computed temperature and density profiles (red curves). It is found that the evolved core ion temperature is much lower than the temperature scaled from DIII-D experiment, and the ITB disappeared, suggesting that the performance goal of Q=5 is unattainable.
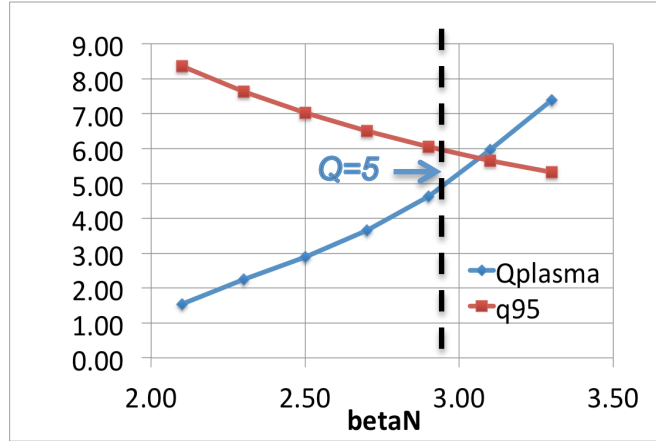
FIG. 9. Extrapolation of DIII-D high β_P scenario to ITER steady state using 0-D model, where the vertical dashed line shows the expected Q=5 operating point.
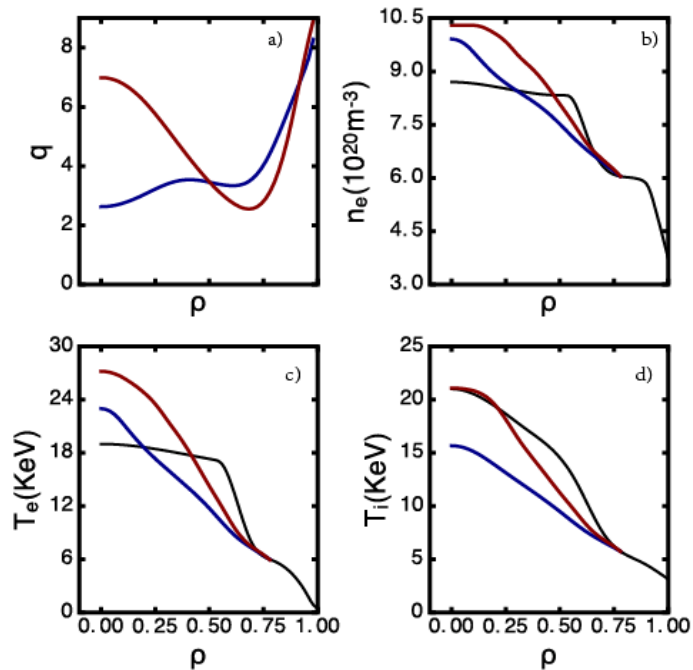
FIG. 10. Comparison of n_e, T_e, T_i evolution of with 1.5-D TGLF-SAT1 model for Q=5 by varying q profile. Black curves are the DIII-D scaled profiles. Red curves are results using the DIII-D q profile; Blue curves with negative central shear q profile.

Further simulations were carried out to investigate the effect of negative central shear on the transport. We increased q(0) by varying of FF', where FF' is the poloidal current function and q(0) is the safety factor on-axis. When q(0) is increased to 7.0 (shown in Figure 10a), the predicted core turbulence is suppressed with the improved core temperature (T_e, T_i) and a predicted fusion performance near Q=5. This improved

confinement is consistent with the Shafranov shift stabilization discussed in Section 3, since increasing to the on-axis safety factor increases the local magnetic shear in the core, similar to the effect of large Shafranov shift.

5. Summary

Recent experiments on DIII-D high beta plasmas with high f_{BS} have demonstrated significant progress towards conditions relevant to steady state Q=5 in ITER. The very high energy confinement quality, $H_{98y2}\sim1.6$, has been maintained when the plasma was evolved towards lower toroidal rotation and q_{95} relevant to steady state operation, although not simultaneously. The excellent confinement is associated with the formation of large radius ITB. Transport analysis and experimental data suggest that the toroidal rotation shear does not provide the dominant effect in the formation of the ITB for the high β_P regime. Further experiments and transport analysis show that Shafranov shift has a key stabilizing effect on the turbulence.

The DIII-D high β_P scenario could be a candidate for ITER steady state operation. When using 0-D model，we found that the Q=5 could be reached at $\beta_N\sim2.9$ and $q_{95}\sim7$ for the extrapolation of the DIII-D high beta scenario ($H_{98y2}\sim1.6$ and $f_{BS}\sim80\%$) towards ITER steady state. Results from 1.5D transport modeling of ITER using TGLF-SAT1 and profile scaled form the DIII-D experiments, show that the confinement falls short of Q=5 at low rotation, but sufficient confinement can be achieved through slightly increasing q(0) with negative central shear for larger negative magnetic shear.

References:
[1] GAROFALO A. *et al* 2015 *Nucl. Fusion* 55 123025
[2] GONG X. *et al* 2014 at the IAEA Int. Conf. on Fusion Energy (St Petersburg, Russia, 13–18 October 2014)
[3] REN Q. *et al* 2016 *phys. Plasma* 23 062511
[4] GORMEZANO C. *et al* 2007 *Nucl. Fusion* 47 S285
[5] GAROFALO A. *et al* 2011 *Nucl. Fusion* 51 083018
[6] CANDY J. 2013 *Phys. Plasma* 16 060704
[7] STAEBLER G.M. 2013 *Nucl. Fusion* 53 113017
[8] CANDY J. *et al* 2003 *J. Comput. Phys.* 186 545
[9] LAO L.L. *et al* 1985 *Nucl. Fusion* 25 1421
[10] BEER M.A. *et al* 1997 *Phys. Plasma 4* 1792
[11] STAMBAUGH R.D *et al* 2011 *Fusion Sci. Tech.*59 279
[12] STAEBLER G.M., http://meetings.aps.org/Meeting/DPP15/Session/To6.14